ARMY RESEARCH LABORATORY

Effects of a Radome on a UWB Detection System

Marc Litz, Romeo D. del Rosario, and Keith Leshick

ARL-SR-73

September 1998

The findings in this report are not to be construed as an official Department of the Army position unless so designated by other authorized documents.

Citation of manufacturer's or trade names does not constitute an official endorsement or approval of the use thereof.

Destroy this report when it is no longer needed. Do not return it to the originator.

Army Research Laboratory

Adelphi, MD 20783-1197

ARL-SR-73 **September 1998**

Effects of a Radome on a UWB Detection System

Marc Litz, Romeo D. del Rosario, and Keith Leshick

Sensors and Electron Devices Directorate

Abstract

We evaluated a radome housing an ultra-wideband (UWB) signal collection system, measuring the transmission loss and phase delay through the radome. The radome introduced losses of up to 3 dB within the normal operating range of the antennas. Phase differences due to the radome appeared to be linear and consistent with the delay expected from a uniformly layered material. We observed no unusual effects from the specially designed protective radome.

Contents

1. Introduction **1**

2. Procedure and Results **2**
2.1 Description of antennas 2
2.2 Description of VNA 2
2.3. Magnitude Measurements 2
2.4 Phase Measurements 5
2.5 Effective Length 5

3. Conclusions **7**

4. Bibliography **7**

Distribution **19**

Report Documentation Page **21**

Appendices

Appendix A.—S-Parameter Magnitude Data **9**

Appendix B.—Gain Curves **15**

Figures

1. Sketch of UWB transportable antennas 1
2. Frequency ranges of UWB transportable antennas 2
3. Diagram of experimental setup 2
4. The transmission loss (S21) for the TEM V2 horn is shown for both configurations, radome on and off 3
5. The transmission loss (S21) for the AEL pyramidal horn is shown for both configurations, radome on and off 3
6. The transmission loss (S21) for the Waveline pyramidal horn is shown for both configurations, radome on and off 4
7. The measured loss through the radome is shown for the three antennas in the wideband collection system 4
8. The measured phase difference caused by the radome is shown 5
9. Effective length of TEM V2 antenna 3
10. Effective length of the AEL 2–18 GHz ridged horn 3
11. Effective length of the Waveline 18–26 GHz standard gain horn 4

1. Introduction

An ultra-wideband (UWB) detection system was developed in response to a growing need to better evaluate the signatures of a wide variety of unintended electromagnetic emanations. The use of this system in the field imposes several design constraints, such as light weight, compactness, and weatherproofing. Moreover, since the vast majority of antennas are narrowband, most radomes are also narrowband. Thus, the uniqueness of this particular design necessitates study.

We measured the transmission loss and phase delay of the specially designed radome for use with the UWB transportable collection system. The radome protects a set of four antennas that cover the frequency range of 50 MHz to 40 GHz in this UWB impulse receiving system. The four antennas consist of a 50-MHz to 2-GHz resistively loaded horn, a 2- to 18-GHz ridged waveguide horn, a standard gain 18- to 26-GHz horn, and a standard gain 26- to 40-GHz horn.

The test configuration consisted of a matched pair of each type of antenna, one mounted standalone and the other mounted inside the collection system. Measurements were taken with and without the radome in place (see fig. 1). The measurements were made inside a $50 \times 25 \times 25$ ft anechoic chamber. (Note: the transverse electromagnetic (TEM) V2 antenna points in the opposite direction from the rest of the UWB transportable antennas.)

The phase and magnitude of the system's three lowest frequency antennas (45 MHz to 26 GHz) were measured with the Hewlett-Packard (HP) 8510C vector network analyzer.

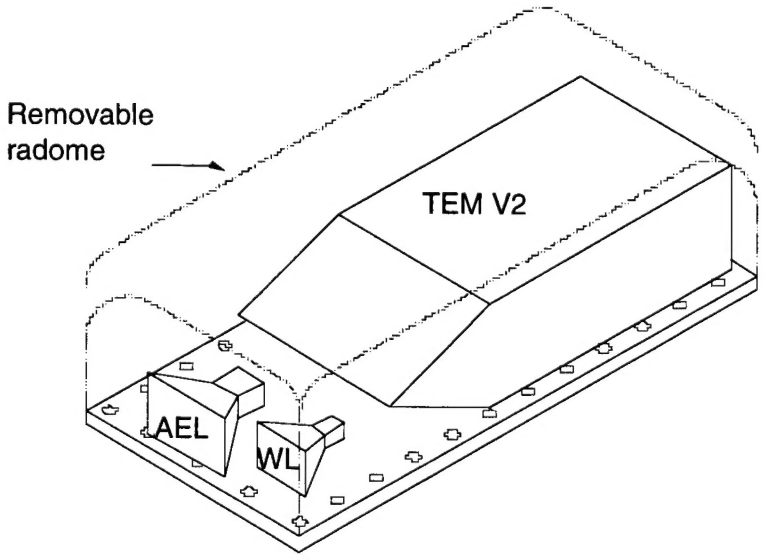

Figure 1. Sketch of UWB transportable antennas.

2. Procedure and Results

2.1 Description of antennas

The antennas contained in the UWB transportable detection system include the (AEL) ridged waveguide horn, the Waveline standard gain horn, and the TEM V2 ultra-wideband resistively loaded horn. Their operational frequencies are displayed in figure 2.

2.2 Description of VNA

We configured the HP8510C vector network analyzer with a two-port, *N*-type test set and a synthesized sweep oscillator with a range from 10 MHz to 26.5 GHz (see fig. 3).

2.3. Magnitude Measurements

A full two-port calibration was performed to allow storage of all four *S*-parameters. In this setup, S_{11} and S_{22} represent the frequency content of the reflected signals. S_{21} and S_{12} are the transmission loss from one antenna to another. (See appendix A for data.)

The TEM V2 ultra-wideband antennas were placed in the setup at an angle of 0° (boresight) with respect to one another. The range between the antennas was 8.91 m. The connectors were chosen as the range reference

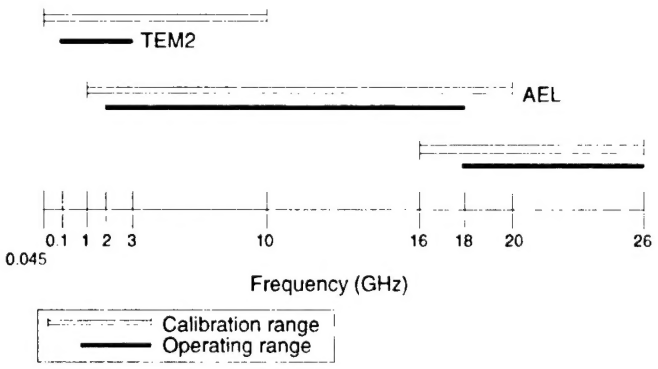

Figure 2. Frequency ranges of UWB transportable antennas.

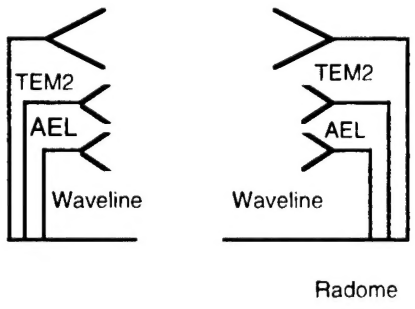

Figure 3. Diagram of experimental setup.

points for all three antennas. In this configuration, we measured the magnitude and phase of the TEM V2 antennas for the frequency range 0.045 to 10 GHz. This procedure was then repeated at the appropriate bands for the AEL and Waveline antennas.

Figures 4 through 6 display the transmission losses for the antenna pairs for both cases, radome on and radome off. Figure 7 illustrates the difference in transmission loss due to the addition of the radome. Within the given operating ranges of the antennas, the radome introduces no more than 3 dB loss. For the TEM V2 antennas, the radome appears to have little effect below 3 GHz. Although the losses appear to exceed 3 dB for frequencies above 3 GHz, the performance is sufficient for the normal operating range of the TEM V2.

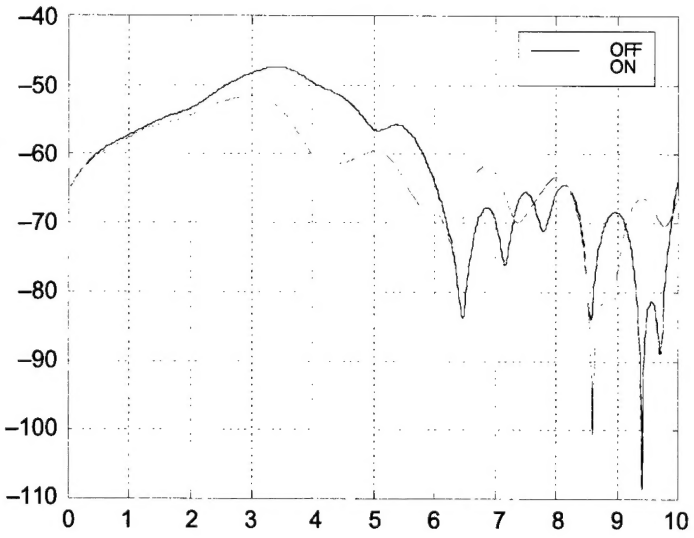

Figure 4. The transmission loss (S21) for the TEM V2 horn is shown for both configurations, radome on and off.

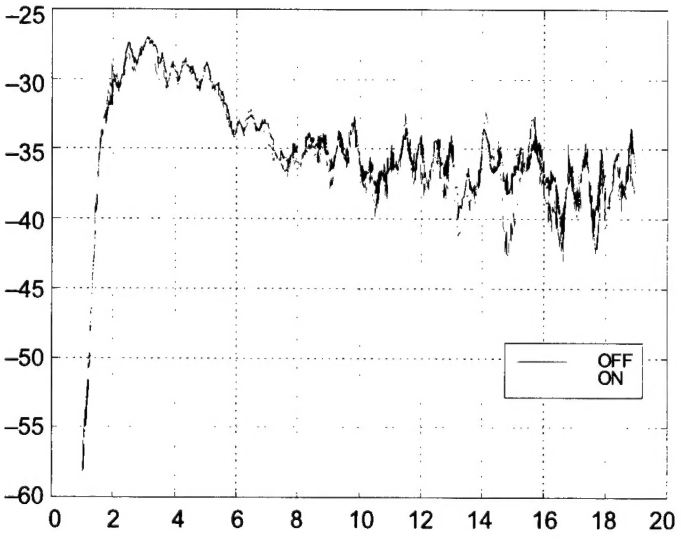

Figure 5. The transmission loss (S21) for the AEL pyramidal horn is shown for both configurations, radome on and off.

The losses increase in direct proportion to frequency for all three antennas. The exception to this occurs at approximately 20 GHz, which may be attributed to a $l/4$ resonance of the radome's thickness of 2.5 mm. Moreover, the S_{12} of the Waveline antenna is different from its S_{21}, indicating that the setup should be verified at these frequencies and the measurement should be repeated.

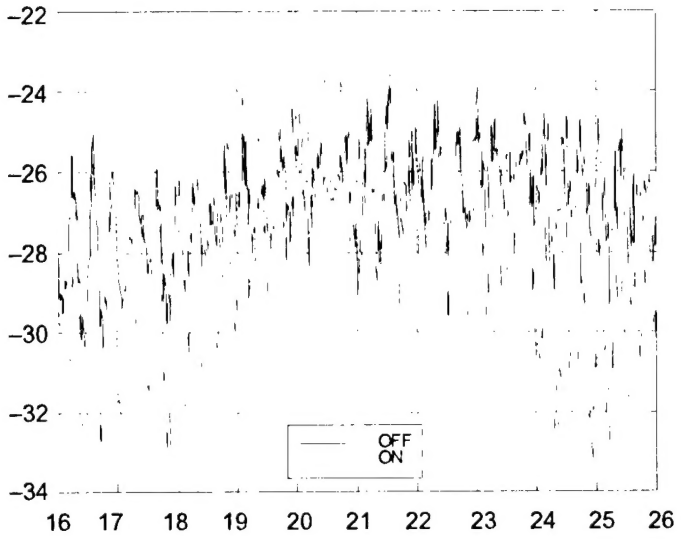

Figure 6. The transmission loss (S21) for the Waveline pyramidal horn is shown for both configurations, radome on and off.

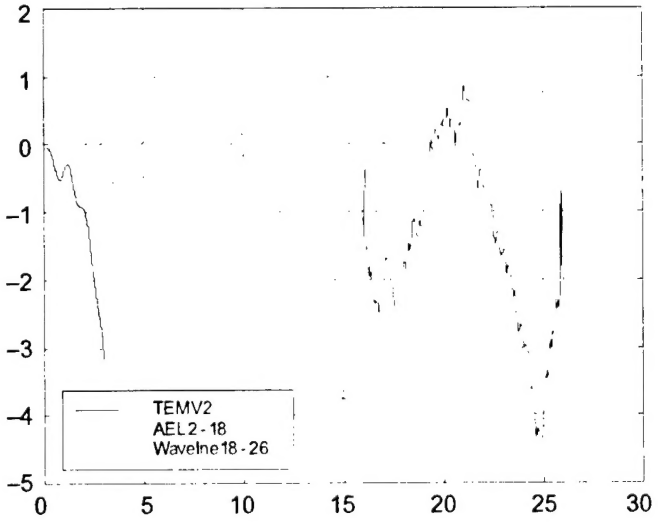

Figure 7. The measured loss through the radome is shown for the three antennas in the wideband collection system.

2.4 Phase Measurements

Phase was measured concurrently with the magnitude of the *S*-parameters. Figure 8 displays the phase difference between radome on versus radome off for all three antennas within their operating ranges.

The difference between the phase measurements indicates any frequency-dependent delay due to the addition of the radome that may contribute to dispersion. The phase of all three antennas is continuous, a highly desirable characteristic for reproducing an impulse. Also, the phase differences are consistent with the delay expected from a uniformly layered material and are fairly linear across antenna operating ranges.

2.5 Effective Length

Figures 9 through 11 display the calculated effective length for each of the antennas based on the S_{21} measurements. An antenna's effective length, $E = V_{rec}/L_{eff}$, relates the electric field incident on the antenna to the voltage measured at the input/output of the antenna (i.e., the voltage that would be observed on an oscilloscope connected to the receive antenna.) This conversion factor will be applied and included with the total calibration factor for the information channel of the UWB transportable collection system. Other parameters that will be recorded for the unit's overall calibration include channel attenuation/amplification and cable losses.

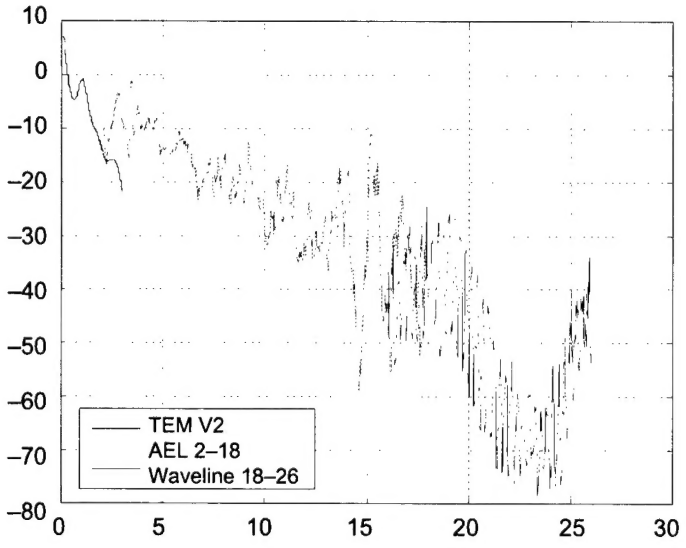

Figure 8. The measured phase difference caused by the radome is shown. The results of all three antennas housed in the system are shown. The three antennas are the TEM horn (100 MHz–3 GHz), AEL horn (2–18 GHz), and the Waveline horn (18–35 GHz).

Figure 9. Effective length of TEM V2 antenna.

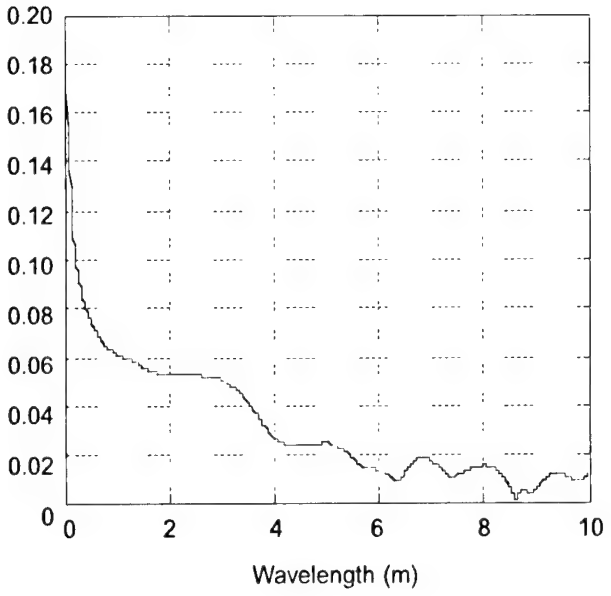

Figure 10. Effective length of the AEL 2–18 GHz ridged horn.

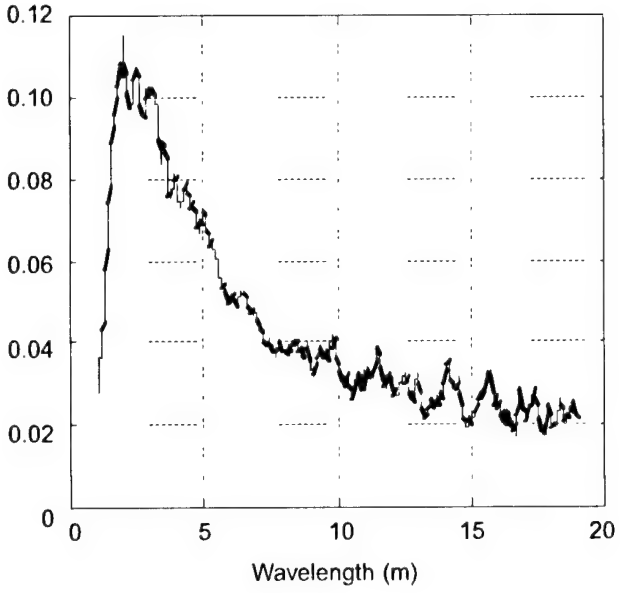

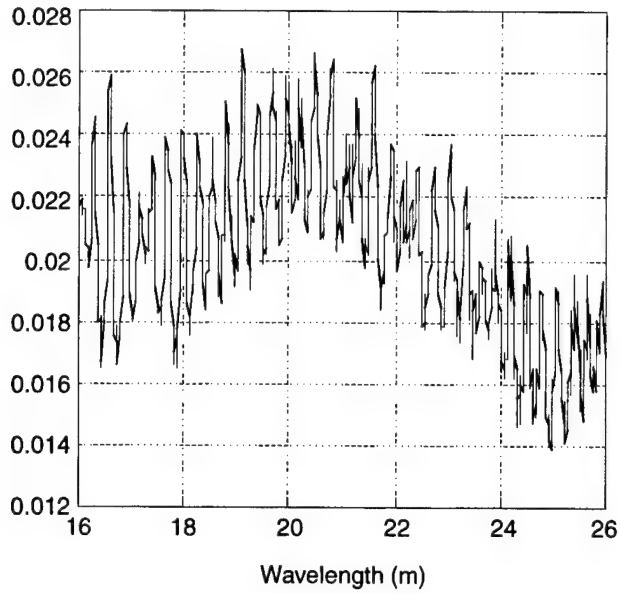

Figure 11. Effective length of the Waveline 18–26 GHz standard gain horn.

3. Conclusions

This evaluation of the radome shows 3-dB variations from 2 to 3 GHz and 10-dB variations from 3 to 5 GHz on the TEM V2 antenna. However, the observed losses from the radome for the TEM V2 antenna are out of the nominal operating range of the antenna in this configuration (above 2 GHz). Likewise, the radome exhibits losses of about 3 dB or less at frequencies from 2 to 24 GHz, which are covered by the AEL and Waveline antennas.

The calculations assume two identical antennas under evaluation, which is not strictly true in these experiments. The antennas in LS support structure should show coupling effects and losses not found in the singular transmitting antennas used in the chamber to complete the pair. (This may account for the differences between S_{11} and S_{22} for given antenna pairs.) Moreover, some future measurements should be performed on an outdoor antenna range since the anechoic chamber is practically limited to frequencies above 150 MHz. Nonetheless, initial results indicate that the radome has sufficiently low insertion loss and delay to make it useful for its intended application.

4. Bibliography

J. D. Taylor, Introduction to Ultra-Wideband Radar Systems, CRC Press, 1995.

M. Morgan, *Optimized TEM Horn Impulse Receiving Antenna*, Naval Post-Graduate School, 1996.

J. D. Kraus, *Antennas*, McGraw-Hill, 1950.

Appendix A.—S-Parameter Magnitude Data

Figure A-1. TEM V2 raw data with and without radome 11
Figure A-2. TEM V2 derivative of two-port phase measurement 11
Figure A-3. AEL raw data with and without radome 12
Figure A-4. AEL 2–18 GHz two-port phase measurement 12
Figure A-5. Waveline 18–26 GHz raw data with and without radome 13
Figure A-6. Waveline 18–26 GHz derivative of the two-port phase measurement 13

Figure A-1. TEM V2 raw data with and without radome.

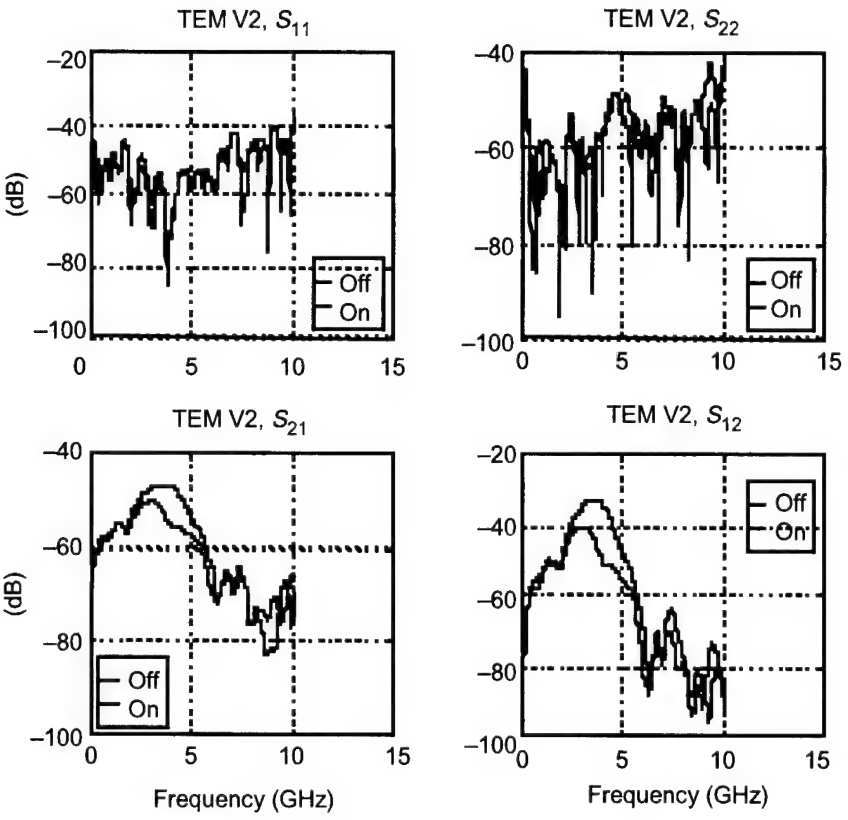

Figure A-2. TEM V2 derivative of two-port phase measurement.

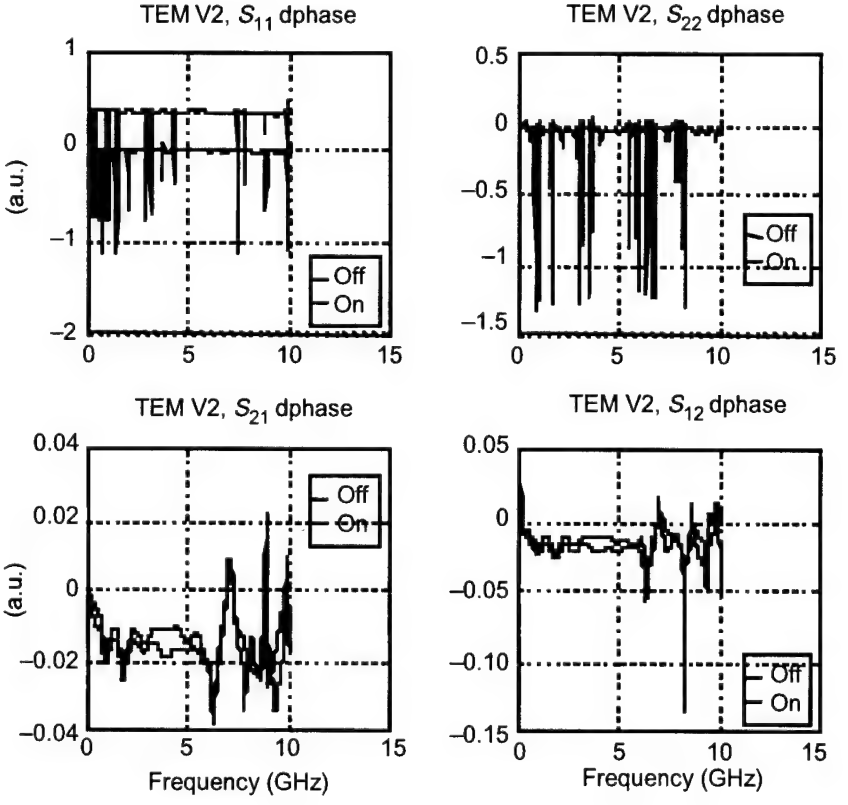

Figure A-3. AEL raw data with and without radome.

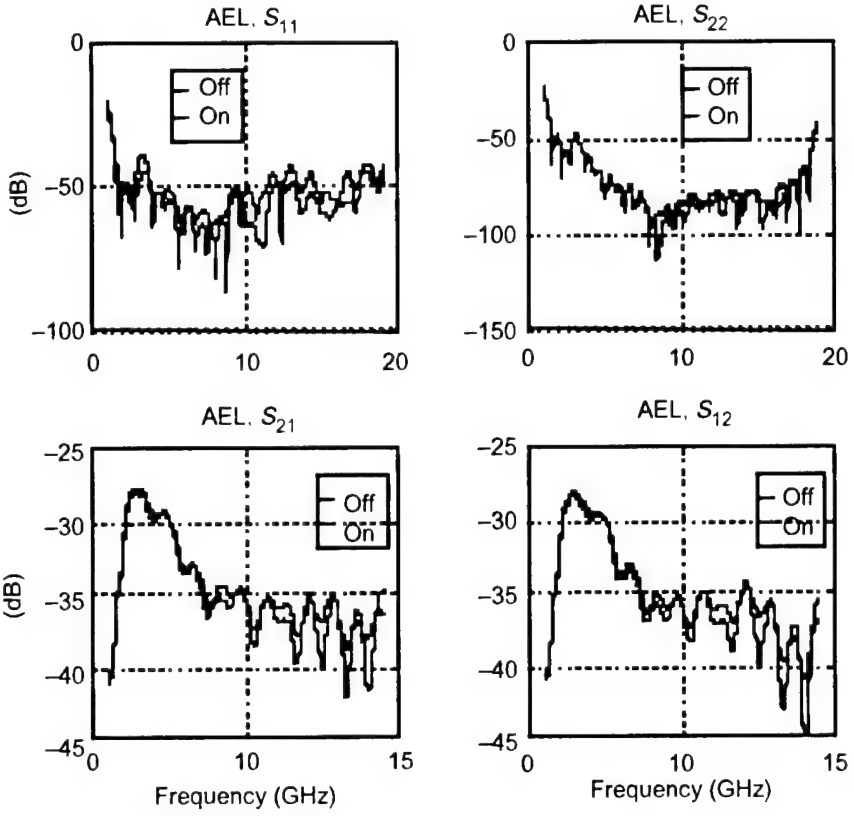

Figure A-4. AEL 2–18 GHz two-port phase measurement.

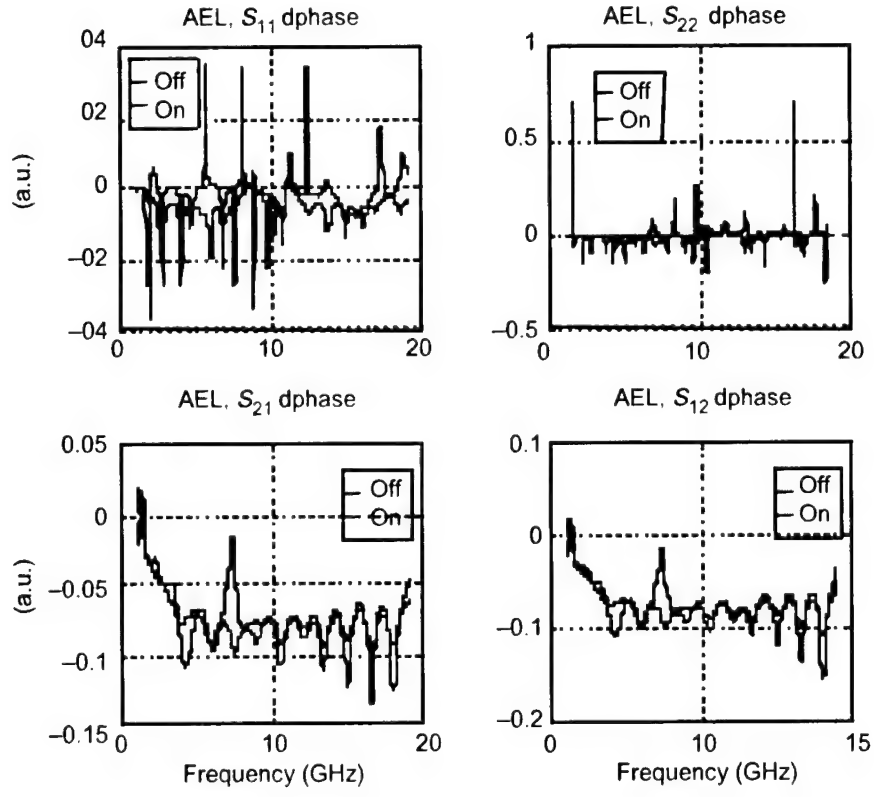

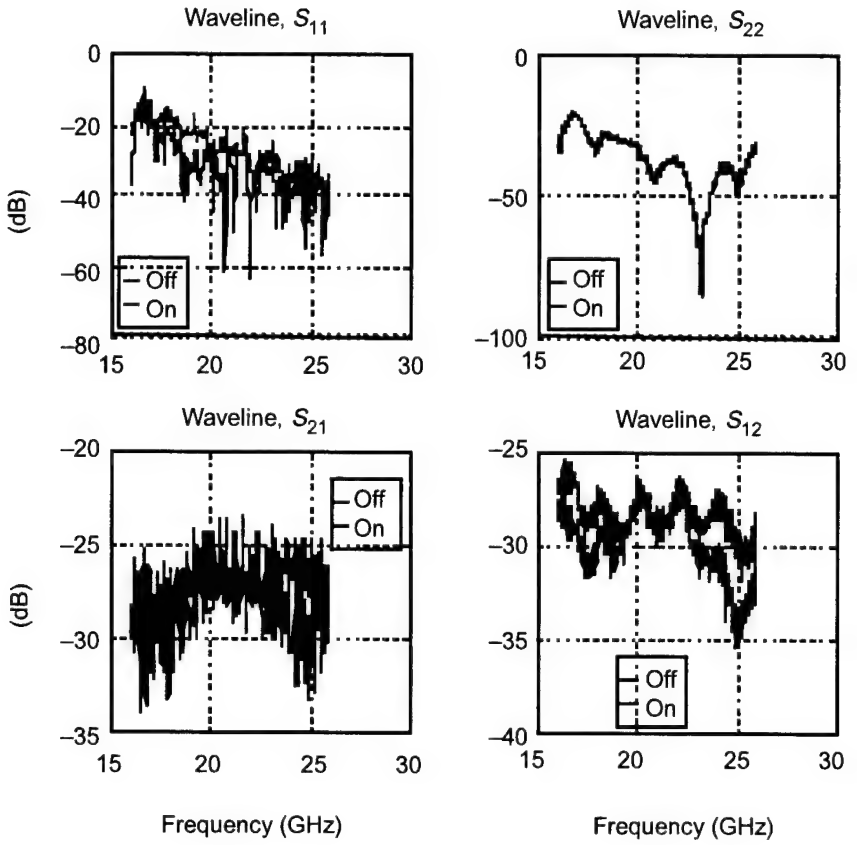

Figure A-5. Waveline 18–26 GHz raw data with and without radome.

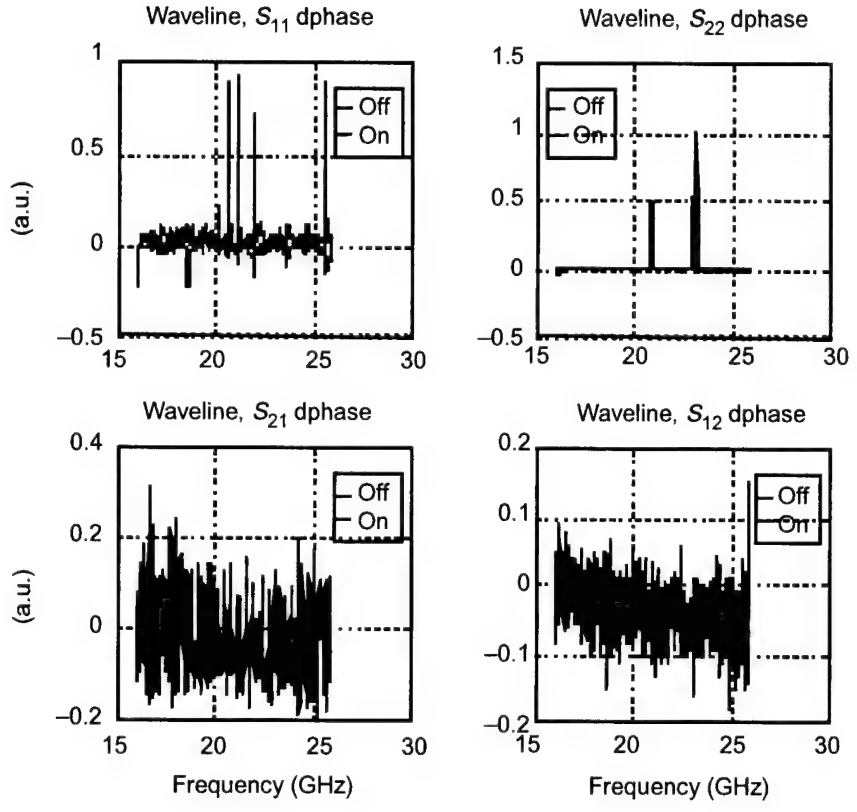

Figure A-6. Waveline 18–26 GHz derivative of the two-port phase measurement.

Appendix B.—Gain Curves

Figure B-1. Gain curve for TEM V2 horns with radome 17
Figure B-3. Gain curve for waveline horns with radome 17
Figure B-2. Gain curve for AEL horns with radome 17

The primary reason for calculating the gain curves was to compare the standard gain (15 dBi) expected from the Waveline to the measured value. Because the receive antenna was located on a metal base (ultra-wideband transportable chassis) adjacent to other receive horns, some coupling between horns was expected and, consequently, we predicted a gain lower than 15 dBi.

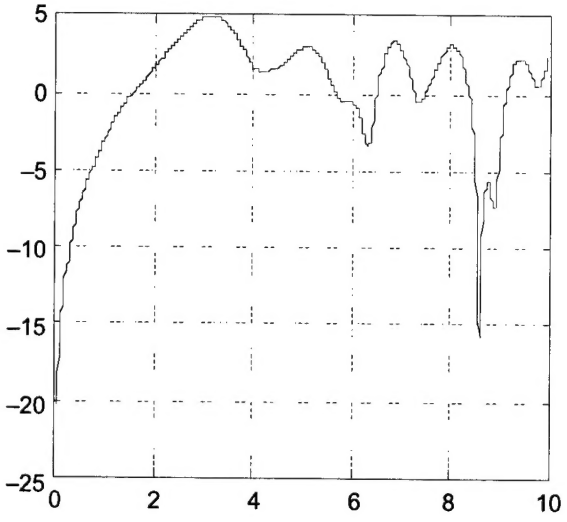

Figure B-1. Gain curve for TEM V2 horns with radome (mounted in LS).

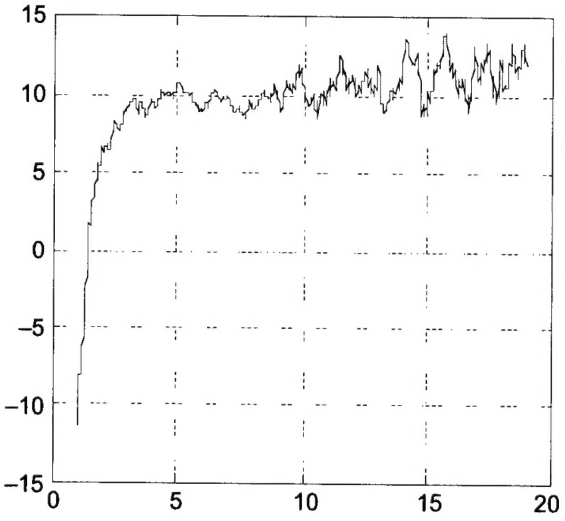

Figure B-2. Gain curve for AEL horns with radome.

Figure B-3. Gain curve for waveline horns with radome.

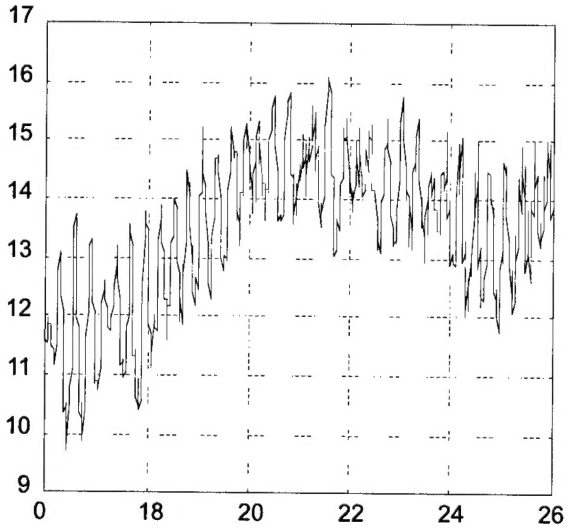

Distribution

Admnstr
Defns Techl Info Ctr
Attn DTIC-OCP
8725 John J Kingman Rd Ste 0944
FT Belvoir VA 22060-6218

Ofc of the Dir Rsrch and Engrg
Attn R Menz
Pentagon Rm 3E1089
Washington DC 20301-3080

Ofc of the Secy of Defns
Attn ODDRE (R&AT) G Singley
Attn ODDRE (R&AT) S Gontarek
The Pentagon
Washington DC 20301-3080

OSD
Attn OUSD(A&T)/ODDDR&E(R) R Tru
Washington DC 20301-7100

AMCOM MRDEC
Attn AMSMI-RD W C McCorkle
Redstone Arsenal AL 35898-5240

Army Rsrch Ofc
Attn AMXRO-GS Bach
PO Box 12211
Research Triangle Park NC 27709

CECOM
Attn PM GPS COL S Young
FT Monmouth NJ 07703

CECOM RDEC Elect System Div Dir
Attn J Niemela
FT Monmouth NJ 07703

CECOM
Sp & Terrestrial Commctn Div
Attn AMSEL-RD-ST-MC-M H Soicher
FT Monmouth NJ 07703-5203

Dir for MANPRINT
Ofc of the Deputy Chief of Staff for Prsnnl
Attn J Hiller
The Pentagon Rm 2C733
Washington DC 20301-0300

Hdqtrs Dept of the Army
Attn DAMO-FDT D Schmidt
400 Army Pentagon Rm 3C514
Washington DC 20301-0460

US Army CECOM Rsrch, Dev, & Engrg Ctr
Attn R F Giordano
FT Monmouth NJ 07703-5201

US Army Edgewood Rsrch, Dev, & Engrg Ctr
Attn SCBRD-TD J Vervier
Aberdeen Proving Ground MD 21010-5423

US Army Info Sys Engrg Cmnd
Attn ASQB-OTD F Jenia
FT Huachuca AZ 85613-5300

US Army Materiel Sys Analysis Agency
Attn AMXSY-D J McCarthy
Aberdeen Proving Ground MD 21005-5071

US Army Natick Rsrch, Dev, & Engrg Ctr
Acting Techl Dir
Attn SSCNC-T P Brandler
Natick MA 01760-5002

Dir US Army Rsrch Ofc
4300 S Miami Blvd
Research Triangle Park NC 27709

US Army Simulation, Train, & Instrmntn Cmnd
Attn J Stahl
12350 Research Parkway
Orlando FL 32826-3726

US Army Tank-Automtv & Armaments Cmnd
Attn AMSTA-AR-TD C Spinelli
Bldg 1
Picatinny Arsenal NJ 07806-5000

US Army Tank-Automtv Cmnd Rsrch, Dev, & Engrg Ctr
Attn AMSTA-TA J Chapin
Warren MI 48397-5000

US Army Test & Eval Cmnd
Attn R G Pollard III
Aberdeen Proving Ground MD 21005-5055

Distribution (cont'd)

US Army Train & Doctrine Cmnd
Battle Lab Integration & Techl Dirctrt
Attn ATCD-B J A Klevecz
FT Monroe VA 23651-5850

US Military Academy
Dept of Mathematical Sci
Attn MAJ D Engen
West Point NY 10996

USAASA
Attn MOAS-AI W Parron
9325 Gunston Rd Ste N319
FT Belvoir VA 22060-5582

Nav Surface Warfare Ctr
Attn Code B07 J Pennella
17320 Dahlgren Rd Bldg 1470 Rm 1101
Dahlgren VA 22448-5100

GPS Joint Prog Ofc Dir
Attn COL J Clay
2435 Vela Way Ste 1613
Los Angeles AFB CA 90245-5500

DARPA
Attn B Kaspar
Attn L Stotts
3701 N Fairfax Dr
Arlington VA 22203-1714

ARL Electromag Group
Attn Campus Mail Code F0250 A Tucker
University of Texas
Austin TX 78712

Palisades Inst for Rsrch Svc Inc
Attn E Carr
1745 Jefferson Davis Hwy Ste 500
Arlington VA 22202-3402

US Army Rsrch Lab
Attn AMSRL-CI-LL Techl Lib (3 copies)
Attn AMSRL-CS-AL-TA Mail & Records Mgmt
Attn AMSRL-CS-AL-TP Techl Pub (3 copies)
Attn AMSRL-SE-DE L Libelo
Attn AMSRL-SE-DP C Lazard
Attn AMSRL-SE-DP D Judy
Attn AMSRL-SE-DP M Litz (10 copies)
Attn AMSRL-SE-DP R A Kehs
Attn AMSRL-SE-DP R del Rosario
Attn AMSRL-SE-DS R Kaul
Attn AMSRL-SE-RU J McCorkle
Adelphi MD 20783-1197

REPORT DOCUMENTATION PAGE

Form Approved
OMB No. 0704-0188

1. AGENCY USE ONLY *(Leave blank)*	2. REPORT DATE	3. REPORT TYPE AND DATES COVERED
	September 1998	Summary, 11/96–5/97

4. TITLE AND SUBTITLE Effects of a Radome on a UWB Detection System

5. FUNDING NUMBERS

DA PR:
PE: 62120A

6. AUTHOR(S) Marc Litz, Romeo D. del Rosario, and Keith Leshick

7. PERFORMING ORGANIZATION NAME(S) AND ADDRESS(ES)
U.S. Army Research Laboratory
Attn: AMSRL-SE-DP email: litz@arl.mil
2800 Powder Mill Road
Adelphi, MD 20783-1197

8. PERFORMING ORGANIZATION REPORT NUMBER
ARL-SR-73

9. SPONSORING/MONITORING AGENCY NAME(S) AND ADDRESS(ES)
U.S. Army Research Laboratory
2800 Powder Mill Road
Adelphi, MD 20783-1197

10. SPONSORING/MONITORING AGENCY REPORT NUMBER

11. SUPPLEMENTARY NOTES
ARL PR: 7NXT69
AMS code: 622120.H16

12a. DISTRIBUTION/AVAILABILITY STATEMENT Approved for public release; distribution unlimited.

12b. DISTRIBUTION CODE

13. ABSTRACT *(Maximum 200 words)*

We evaluated a radome housing an ultra-wideband (UWB) signal collection system, measuring the transmission loss and phase delay through the radome. The radome introduced losses of up to 3 dB within the normal operating range of the antennas. Phase differences due to the radome appeared to be linear and consistent with the delay expected from a uniformly layered material. We observed no unusual effects from the specially designed protective radome.

14. SUBJECT TERMS
Ultra-wideband, antenna

15. NUMBER OF PAGES
21

16. PRICE CODE

17. SECURITY CLASSIFICATION OF REPORT	18. SECURITY CLASSIFICATION OF THIS PAGE	19. SECURITY CLASSIFICATION OF ABSTRACT	20. LIMITATION OF ABSTRACT
Unclassified	Unclassified	Unclassified	UL

NSN 7540-01-280-5500

Standard Form 298 (Rev. 2-89)
Prescribed by ANSI Std. Z39-18
298-102